Detailed safety assessment for the VVER-1000 fuel assembly

Mohamed Y.M. Mohsen and
Mohamed A.E. Abdel-Rahman*

Nuclear Engineering Department,
Military Technical College,
Kobry Elkobbah,
Cairo, Egypt
Email: moh39333@mtc.edu.eg
Email: mabdelrahman@mtc.edu.eg
*Corresponding author

Abstract: This paper presents three main studies for one fuel assembly of the VVER-1000. The first study is the neutronic analysis using MCNPX. The second study is the thermal-hydraulic analysis. The third study is the solid mechanics analysis by using COMSOL-Multiphysics. The sequence of the above studies is set as follows: during the neutronic analysis, the main safety related parameters, fuel burn-up calculations and the power mapping are simulated. The analytical solution of the thermal-hydraulic revealed that, the maximum fuel and clad temperatures are 1398.9 K and 653.95 K, respectively. Finally, the solid mechanics analysis revealed that the maximum von Mises stress acting on both the fuel and clad materials are 91.81 MPa and 40.82 MPa, respectively, and the maximum fuel outer surface displacement equals to 0.06023 mm. The results obtained from this paper are in a good agreement with both the FSAR and the previous published works.

Keywords: VVER-1000; MCNPX; neutronic analysis; thermal-hydraulic analysis; solid mechanics analysis; PPF; hot channel; MATLAB; COMSOL-Multiphysics; MDNBR; FSAR.

Reference to this paper should be made as follows: Mohsen, M.Y.M. and Abdel-Rahman, M.A.E. (2021) 'Detailed safety assessment for the VVER-1000 fuel assembly', *Int. J. Nuclear Energy Science and Technology*, Vol. 15, No. 1, pp.36–60.

Biographical notes: Mohamed Y.M. Mohsen obtained his BSc degree of Nuclear Engineering from the department of Nuclear Engineering at the Military Technical College (MTC), Cairo, Egypt in 2016. Currently, he is pursuing his PhD degree in the same department. His research interests include the utilisation of different codes to investigate the nuclear reactor core, such as MCNPX code, COMSOL-Multiphysics and MATLAB software (with a particular emphasis on VVER-1000 and AP-1000 reactor core).

Mohamed A.E. Abdel-Rahman obtained his PhD degree in Nuclear and Radiation Engineering from the University of Surrey, UK in 2011. His research interests include neutron gamma spectrometer, design of shielding barriers against ionising radiation, radiation protection of all types of ionising radiations, measurements of naturally occurring radioactive materials,

and analysis of core configuration of a nuclear power plant during the following years. He was appointed as Assoc. Professor in nuclear and radiation engineering in 2017. He is currently the head of Nuclear Engineering department in Military Technical College (MTC), Cairo, Egypt.

1 Introduction

Water-Water Energetic Reactor (WWER) or (VVER) is a pressurised water reactor with thermal neutrons. VVER design consists of two horizontal steam generators with four coolant loops, main circulation pump, pressuriser, relief and emergency valves on steam pipes and accumulator tanks for the Emergency Core Cooling System (ECCS) (ROSATOM, 2020). VVER power stations are widespread as they are installed, not only in Russia, but also in China, Finland, Germany, Hungary, Slovakia, Bulgaria, India and Iran. Additionally, there are countries like Bangladesh, Egypt, Jordan and Turkey that are seeking to introduce VVER reactors (Wikipedia, 2020).

Our case study is the Iranian VVER-1000 pressurised water reactor that developed by ROSATOM after 1975 and their thermal and electrical powers are about 3120 MW_{th} and 1000 MW_{ele} respectively with 32.05% thermal efficiency for its Rankine cycle (Arshi et al., 2010). Its design belongs to generation III of the nuclear power reactors. Its core design consists of 163 hexagonal fuel assemblies. Each fuel assembly contains 331 positions distributed in a hexagonal array. These positions are occupied accordingly, 311 positions for fuel rods, 18 empty guide tubes which can be occupied by (control rods, fuel rods with Burnable Absorbers (BAs) and instrumentation tubes), one central guide tube and one measurement guide tube. In the reactor core there are three patches of enrichment; 1.6%, 2.4% and 3.6% (Arshi et al., 2010; Faghihi and Mohammad, 2011).

The main objective of our study is to get a very high accurate prediction for the neutronic, thermal-hydraulic and solid mechanics analysis for one of the central fuel assemblies with 2.4% U^{235} enrichment. As known, the three previous studies play a vital rode in the reactor design, safety and control. From the neutronic analysis, the reactivity calculations, the fuel burn-up and neutron flux and power distribution have been calculated. The aims of the thermal-hydraulic analysis are to make sure that the maximum temperatures of the fuel, clad and coolant as well as the Minimum Departure from Nucleate Boiling Ratio (MDNBR) distribution along z-axis do not exceed the safety limits that are mentioned in the Final Safety Analysis Report (FSAR). The solid mechanics analysis was used to make sure that the maximum von Mises stress acting on both the fuel and clad material doesn't exceed the yield stress for these materials. In addition, the volumetric strain for both fuel and clad materials would not cause any surface contact between fuel and the clad to avoid chemical interactions.

The coupling between the thermal-hydraulic and solid mechanics analysis using COMSOL-Multiphysics is one of the most developed techniques to obtain a very high accurate prediction for the thermal-hydraulic and solid mechanics results. The obtained results have been compared with both the previously published works that used different codes for calculations (WIMS D-4 and CITATION for neutronic analysis and COPERA-EN code for thermal-hydraulics analysis) (Arshi et al., 2010) and with the final safety analysis report for Iranian VVER-1000.

2 Methodology

2.1 MCNPX modelling and simulation

Monte Carlo N-Particle X MCNPX version 26f with ENDF/BVII nuclear data libraries was used for modelling and simulation the neutronic analysis based on the Monte Carlo algorithm (McKinney, 2011).

2.1.1 Geometry cards (cell and surface cards)

One of the central fuel assemblies of the VVER 1000 with enrichment 2.4% was chosen to perform our neutronic calculations as shown in Figure 1. The core of the VVER 1000 consists of 163 fuel assemblies collected together in a hexagonal matrix. These fuel assemblies are distributed in three batches of enrichment (1.6%, 2.4% and 3.6%). Each fuel assembly consists of 331 positions. These positions are occupied with 311 fuel rods of specific enrichment, 18 empty guide tubes; which can be occupied by control rods, fuel rods with BAs and instrumentation tubes, one central guide tube and one measurement guide tube. The fuel rods are of the type annular pin cooled outside only. The design parameters of the VVER-1000 fuel assembly are listed in Table 1 (Arshi et al., 2010; Faghihi and Mohammad, 2011).

Table 1 The design parameters of the VVER-1000 fuel assembly

Reactor core			*Fuel rod*		
Parameters	*units*	*value*	*Parameters*	*units*	*value*
Assembly array	–	Hexagonal array 331 positions	Internal cavity diameter	mm	1.5
Number of UO_2 fuel rods	–	311	Fuel pellet diameter	mm	7.57
Number of guide tubes	–	18	Clad inside diameter	mm	7.73
Number of instrumentation tube	–	1	Cladding material outer diameter	mm	9.1
Number of central guide tube	–	1	Guide tubes & instrumentation tube		
Assembly pitch	cm	23.5	Water inner radius	cm	.48
Fuel rod pitch	cm	1.275	Cladding outer radius	cm	.56
Fuel material (UO_2)			*Cladding material*		
Theoretical density (TD)	gm/cm^3	10.96	Alloy Zr + 1% Nb	gm/cm^3	6.55
UO_2 density	gm/cm^3	10.4668 which equal 95.5% of TD			
U^{235} enrichment	wt.%	2.4%			
Active fuel height	cm	355			

Figure 1 Different sections using Visual editor version 12N for (a) Plan view for VVER-1000 fuel rod (b) Plan view for VVER-1000 fuel assembly (c) Side view for VVER-1000 fuel assembly

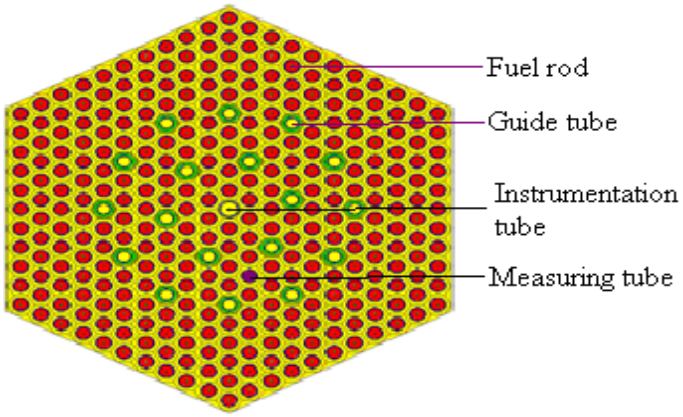

(a)

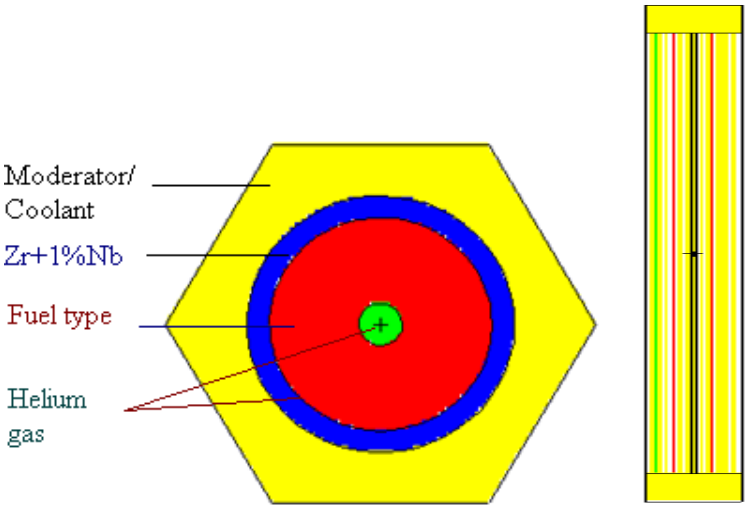

(b) (c)

2.1.2 Material card

In this study, uranium dioxide was used as a fuel material with ^{235}U enriched to 2.4%. The clad material used in VVER-1000 power reactor is of type Alloy (Zr + 1% Nb) which was used to keep the fission fragments away from the coolant. The main reason for choosing (Zr + 1% Nb) as a clad material is its high resistance to corrosion and radiation damage. More specifically (Zr + 1% Nb) mechanical and thermo-physical properties are stable within the operating condition of the VVER-1000. Water is used as a moderator and a coolant, where it used as a moderator for fast neutrons because of its high moderating ratio and used as coolant for the core by transferring the heat from the

core to the steam generators. The helium gas is used to reduce the stress produced due to the emission of the fission products in order to keep the fuel pellet away from swelling. If this swelling occurs, the likelihood of the occurrence of the interactions between the fuel and the clad will increase. Table 2 presents the atomic and weight fraction for the used materials in the MCNPX material card.

Table 2 The composition of the materials used in MCNPX computer code at room temperature 25°C

Uranium dioxide UO_2 (2.42%)		*Clad material*		*Water*		*Helium*	
Isotope	*Atomic fraction*	*Isotope*	*Mass fraction*	*Isotope*	*Mass fraction*	*isotope*	*Mass fraction*
^{235}U	0.000567411	Zr	–0.9811	H-1	–0.1111111	He-4	–1
^{238}U	0.022783249	O-16	–0.0012	O-16	–0.888889		
O-16	0.046703949	Nb-93	–0.01				
		Hf	–0.0003				

2.2 COMSOL-Multiphysics modelling and simulation

2.2.1 Modelling

For the purpose of thermal-hydraulic and solid mechanics simulation, the 2D axisymmetric space dimension has been used to model the fuel rod. The fuel rod type is annular, cooled on the outer surface with only a coolant channel of type hexagonal. The simulation of the hexagonal shape in the 2D axisymmetric is impossible. Therefore, the hydraulic diameter has been calculated to convert the hexagonal coolant channel to cylindrical one by using equation (1). Figure 1 shows the model that used for describing the fuel rod in 2D axisymmetric space dimension.

$$Hydraulic\,diamter = \frac{4 \times A_{flow}}{P} \tag{1}$$

A_{flow} is the cross-sectional area of the coolant flow in m^2 and P is the wetted perimeter of the cross-section in m.

2.2.2 Meshing

Meshing process is the most important step in the numerical solution, this is due to the fact that it plays a vital role in the accuracy of the results. In COMSOL-Multiphysics, the mesh statistics is the tool that used to display the different mesh measures such as skewness. For the skewness, the closer to zero is the better but below 0.8 is considered a good value according to the COMSOL-Multiphysics user guide (COMSOL-Multiphysics, 2020). Table 3 shows the results of skewness and it can be seen that the results are acceptance. Figure 2 presents the mesh quality plot and it's cleared that all mesh qualities for all elements are close to unity.

Table 3 The meshing quality measure

Quality factor	*Minimum*	*Average*	*Condition*
Skewness	0.1979	0.7504	Accepted

Figure 2 The meshing quality plot

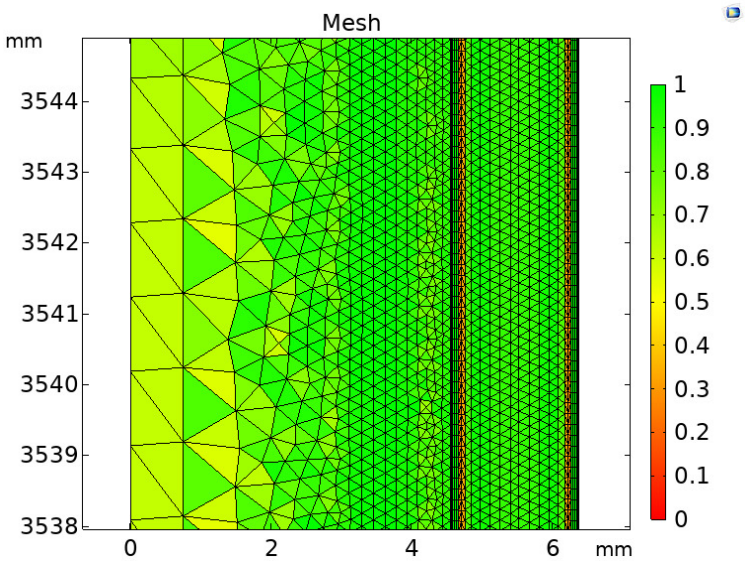

3 Results and discussion

3.1 Neutronic analysis results

3.1.1 Reactivity results

The reactor reactivity calculations have been studied to demonstrate the behaviour of the reactor due to any dynamic change during the normal operational conditions. These dynamic changes may occur due to the neutronic or the thermal-hydraulics effects such as the fuel temperature change, moderator temperature change, boron concentration, control rod motion, fuel burn-up, xenon and samarium build-up and the heat removal system capability. Equation (2) has been used to calculate the reactor reactivity feedback after any change in the main reactor parameters (Lamarsh, 2020).

$$\rho = \frac{K_{eff} - 1}{K_{Eff}} \tag{2}$$

By differentiating equation (2), the temperature coefficient has been determined as shown in equation (3)

$$\alpha(T) = \frac{1}{K_{Eff}^2} \times \frac{dK_{eff}}{dT} \text{ (Lamarsh, 2020)} \tag{3}$$

The temperature feedback and the temperature coefficient for both the fuel and moderator materials have been computed as shown in Table 4.

Table 4 Results for the temperature feedback and coefficients for fuel and moderator materials

Parameter	*The obtained results*
Fuel temperature feedback (cent)	–78.46
Moderator temperature feedback (cent)	–101.85
Fuel temperature coefficient (pcm/°C)	–2.09
Moderator temperature coefficient (pcm/°C)	–24.57

To investigate the effect of void fraction on the behaviour of the fuel assembly criticality (K_{inf}), it is assumed that a nucleate boiling problem occurred during operation. This will cause a double phase flow (coolant and voids). The void fraction has an effect on both the thermal-hydraulic analysis (fuel and clad temperature distribution) and on the neutronic analysis (reactivity of the reactor). The coolant channel has been divided into regions with a specific height along *z*-axis, which will be gradually filled with voids instead of water until the coolant channel is fully occupied with voids (dry-out region on the boiling curve). In each step, the K_{inf} is computed for the fuel rod. From a neutronic point of view, an increase in the fuel temperature introduces a negative reactivity, resulting in the reactor being safe. Contrariwise, from a thermo-hydraulic point of view, the double phase causes an increase in both fuel and clad temperatures, which in turn may cause a partial or total core meltdown. It can be deduced from Figure 3 that the multiplication factor of the fuel assembly decreases gradually with the increase of the void volume percentage until –75%. Then, it decreased sharply to reach K_{inf}–1 when the void volume fraction –0.95%. This decrease in the multiplication factor could be due to the decrease in the neutron's moderation probability as the water volume decrease with respect to the increase in the void percentage.

Figure 3 The change of the infinite multiplication factor with the void volume fraction

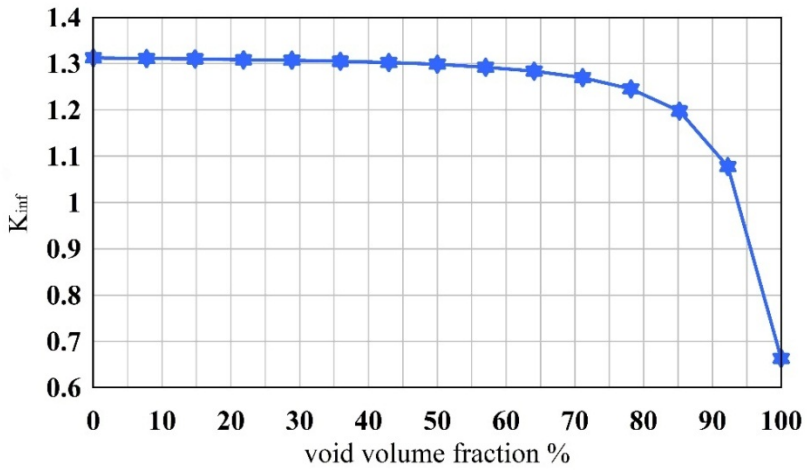

3.1.2 Burn-up calculations

In burn-up calculations, some neutronic characteristics have been determined such as: the fuel cycle length, maximum fuel burn-up, and the inventory of the actinides and non-actinides nuclides along the reactor operational time. Some of these actinides can be used again as s fuel material after reprocessing for the spent fuel such as the remain un burnt U and the produced reactor grade plutonium rgPu. Another type of the actinides is called minor actinides that emit alpha particle and remains in the spent fuel for a long period, therefore, its radioactivity must be taken into consideration in the spent fuel shielding process and storage time such as ^{237}Np and ^{241}Am. The most dominant non-actinides nuclides are the fission products that affect the reactor reactivity such as ^{149}Sm and ^{135}Xe.

Figure 4 presents the fuel assembly reactivity change with the operating times, where the reactor can operate to about 300 days with refuelling with maximum fuel burn-up equal to about 13.75 GWD/MTU. So that for the three cycles of operation, the total fuel burn-up will be about 41.25 GWD/MTU. The obtained results show a good agreement with both the typical value suggested by reference data from FSAR of VVER-1000 reactor, 297.7 days (IAEA, 1995) as well as with the value suggested in previous published work by using WIMS D-4/citation (Faghihi et al., 2016) the burn-up at the end of cycle length is –43 GWD/MTU (Faghihi et al., 2016). In another previous work, the fuel length and the burn-up at the end of fuel cycle were –293.82 days and –34.5 GWD/MTU, respectively (Faghihi et al., 2007). The difference in burn-up results could be due to that the authors used WIMS code which solves the neutron transport equation analytically with approximation.

Figure 4 The infinite multiplication factor change for the fuel assembly with reactor operating time

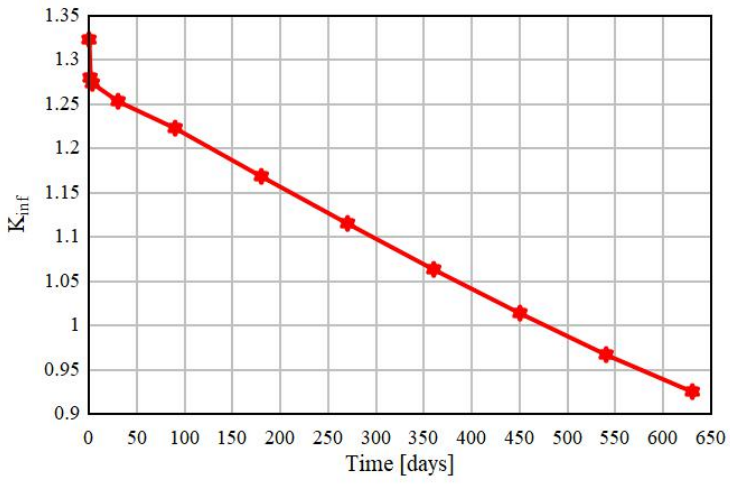

After the reactor is shut down, it is important to determine which materials will be used for shielding the spent fuel storage pool and the time required for storing it safely, until its activity reduced to the allowable limits. Figure 5(a) shows the average assembly production of the reactor grade plutonium along the operational time. The rgPu can be extracted from the spent fuel chemically and then used as a MOX fuel for the pressurised

water reactors. The production of the minor actinides (^{237}Np) along the operational time is shown in Figure 5(b).

Figure 5 The average assembly production of the actinides (a) reactor grade plutonium (rgPu), (b) Neptunium

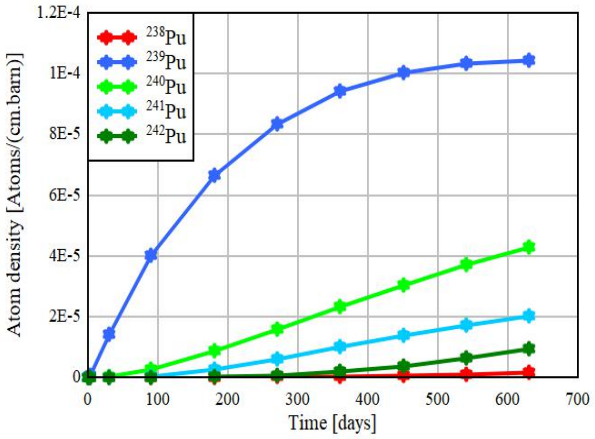

(a)

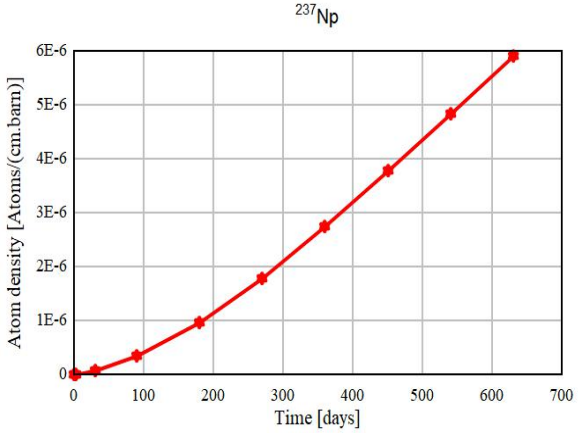

(b)

Figures 6(a) and 6(b) illustrate how the uranium isotopes (^{235}U and ^{238}U) are consumed along the operational time of the fuel assembly due to fuel burn-up. Additionally, at the end of the fuel cycle, there is still about 20% and 98.22% of the initial mass of ^{235}U and ^{238}U, respectively, unburnt. This amount of fuel can be used again as a fuel after making reprocessing process and extracted from the spent fuel.

Figure 6 The average assembly consumption of the actinides (a) ^{235}U and (b) ^{238}U

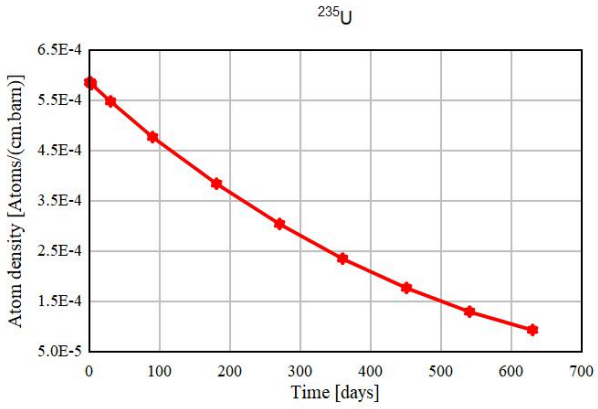

(a)

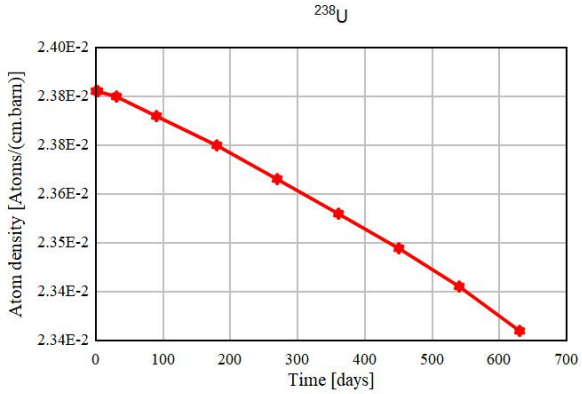

(b)

Figure 7 presents the amount of (^{149}Sm and ^{135}Xe) isotopes that are produced along the operational time of this fuel assembly. ^{149}Sm and ^{135}Xe are considered the most important non-actinides elements that produced during the fuel burn-up process because they have a very high neutron absorption cross section. The production of ^{149}Sm and ^{135}Xe causes negative reactivity and hence, decreases the effective multiplication factor of the fuel assembly. The main aims from studying the production of ^{49}Sm and ^{135}Xe are firstly, this negative reactivity must be compensated by the adding an excess mass of the nuclear fuel material to maintain the sustained chain fission reaction. Secondly, after the reactor power shut down, the negative reactivity resulted from the build-up of the ^{135}Xe and ^{149}Sm in the reactor must be calculated in order to calculate the reactor dead time. This is the time, at which the reactor is unable to overcome the presence of the negative reactivity of ^{135}Xe and ^{149}Sm because at that time the negative reactivity of ^{135}Xe and ^{149}Sm is higher than the positive reactivity of all control rods, when withdraw all of them out of the core. So, this time must pass to reduce the negative reactivity of both ^{135}Xe and

^{149}Sm through the radioactive decay process (both ^{135}Xe and ^{149}Sm become completely burned). After that the reactor can be started again.

Figure 7 The average assembly production of the non-actinides elements (poisons)

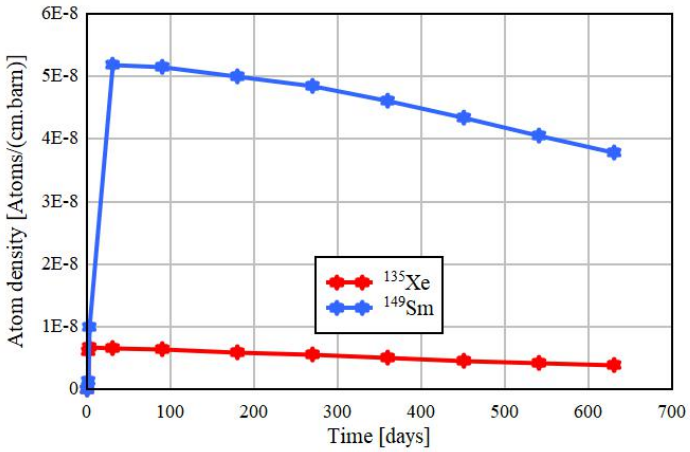

3.1.3 Power mapping results

The main reason behind these calculations is to determine the location of the hot position in the fuel assembly and its corresponding power peaking factor value. The hot channel has been determined by using tallies card in MCNPX computer code. In tallies card, both F4 and FM4 are used for the neutron flux calculation and the normalisation factor respectively. For the neutron flux normalisation factor, equation (4) has been used.

$$\varphi\left[\frac{neutrons}{\text{cm}^2.\text{sec}}\right]=\frac{power[W]\times\bar{\upsilon}\left[\frac{neutrons}{fission}\right]\times\varphi_{F4}\left[\frac{1}{\text{cm}^2}\right]}{E_R[W]\times K_{EFF}} \tag{4}$$

where:

Power is the produced thermal power from any case study such as fuel rod, fuel assembly and the full core.

$\bar{\upsilon}$ the average number of neutrons produced per fission.

φ_{F4} the neutron flux calculated from the tally card F4.

E_R the recovery energy produced from one fission.

Figure 8 shows how the thermal neutron flux changes axially, where the flux is maximum at the centre of the fuel assembly (at Z=0) and decreases with a cosine shape until reach the reflector material (i.e., water in VVER-1000) then it increases again in the reflector region. This increase in the flux is due to the increase in the probability of the elastic interaction that done between the fast neutrons and the hydrogen in water, which will increase the existence of the thermal neutrons in reflector region.

Figure 8 The thermal neutron flux distribution along the axial core distance

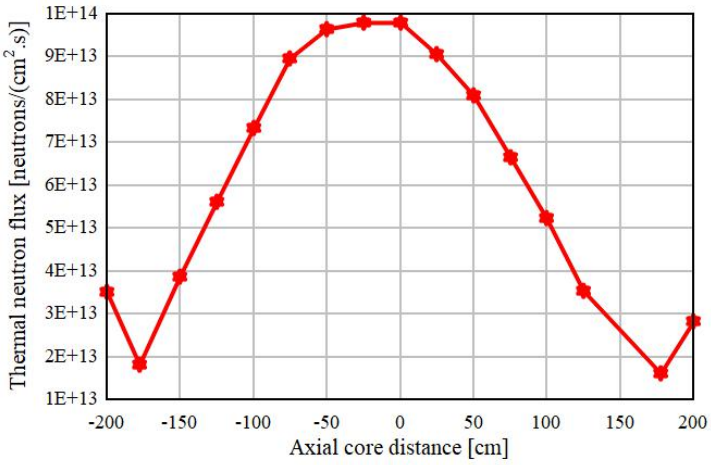

For the power normalisation factor, equation (5) has been used. The nonstandard special *R* numbers –6 and –8 are used for describing the total fission cross section (barn) and recovery energy *Q* (W/fission), respectively.

$$\text{power normalisation factor} = \varphi\left[\frac{\text{neutrons}}{\text{cm}^2.\text{sec}}\right]\times V\left[\text{cm}^3\right] \times\rho\left[\frac{\text{Atoms}}{\text{cm.barn}}\right]\times -6\left[\text{barn}\right]\times -8\left[\frac{\text{W}}{\text{fission}}\right] \tag{5}$$

For calculating the radial PPF distribution, the power generated inside each fuel rod and calculated by MCNPX is divided by the average power produced from each fuel rod. Note that the average power is calculated by dividing the full core thermal power produced by the total number of fuel rods. The hot channel is that one in which the maximum PPF occurred.

Figure 9 presents the power peaking factor distribution for one-sixth of the fuel assembly and the concept of symmetry can be used to model power distribution across the fuel assembly. It can be deduced from Figure 9 that channel number 64, which has power peaking factor 1.285 is the hot channel. In Table 5, a comparison of our obtained results for max PPF with the other published work that used different code (WIMS D-4/citation) for the neutronic calculations was done. It is obvious from Table 5 that the obtained results are consistent with the value suggested by using WIMS D-4/citation (Arshi et al., 2010) (–1.29).

Table 5 Maximum PPF occur at the begin of the fuel cycle (Hot full power state)

Max PPF at (BOC)	*Results using (MCNPX)*	*WIMS D-4/citation (Arshi et al., 2010)*
value	1.285	1.29

Figure 9 Radial power peaking factor distribution for one-six of the fuel assembly at the begin of the fuel cycle

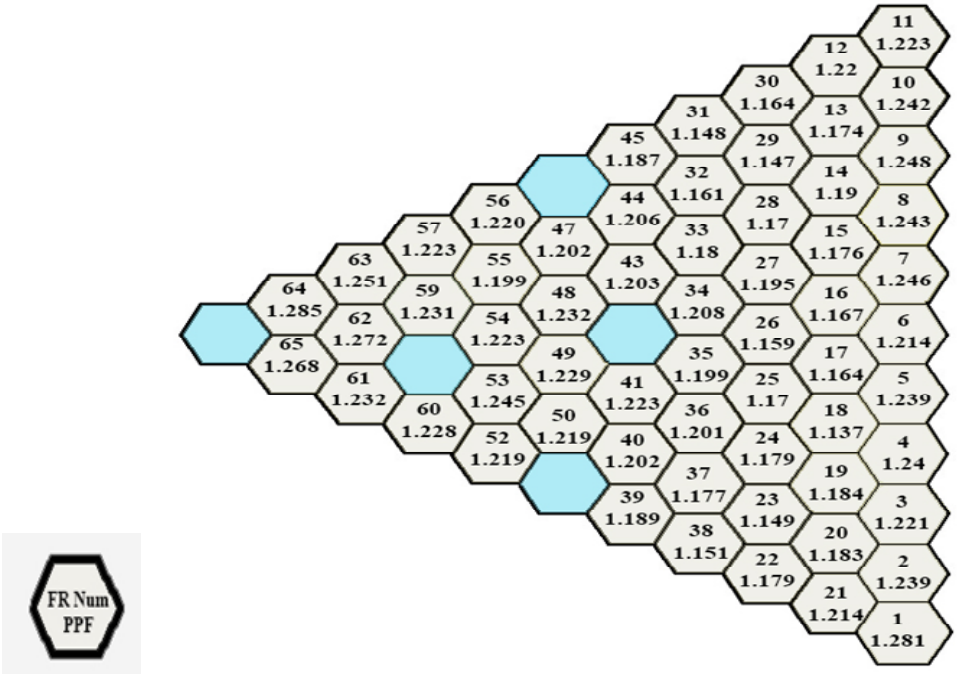

3.2 Thermal-hydraulic results

The thermal-hydraulic analysis starts after determining the hot channel at which the maximum power peaking factor occurs. The aim of the thermal-hydraulic analysis is to obtain the temperature distribution of the fuel, clad and coolant materials and the axial distribution of the Departure from Nucleate Boiling Ratio (DNBR). There are three requirements must be achieved in thermal hydraulic design to achieve the safe design. Firstly, the fuel temperature must be less than its solidus temperature, which is approximately 2873 K. Secondly, the maximum clad temperature must be less than its melting point, 2123 K but if there is a surface contact between the fuel and the clad, the clad temperature must be less than 1135 K to avoid chemical interaction between the clad and the fuel materials. Thirdly, the MDNBR must be higher than 1.75 for PWR to keep the coolant away from nucleate boiling region. In this work, thermal-hydraulic analysis has been conducted using two approaches; analytical approach using MATLAB and numerical approach using COMSOL Multiphysics.

3.2.1 Thermal hydraulic results using analytical approach

The analytical approach was performed using MATLAB (MathWorks, 2020) to solve the heat generation equation (partial differential equation) for the fuel and clad as a closed volume. On the other hand, it was solved as an open volume to get temperature distribution along the coolant. The in-detailed solution of the heat generation partial differential equation for the fuel rod of type annular cooled on the outer surface only

exist in our previously published work (Mohsen et al., 2020) and in Kazimi and Todreas (1990). The average values for the thermo-physical properties of the fuel, clad and coolant materials (thermal conductivity, heat capacity at constant pressure and the density) have been used, as shown in Table 6.

Table 6 Approximated values for the design parameters used for analytical approach

Parameter	*Description*	*Units*	*Values*
k_f	Thermal conductivity of the fuel	(W/m.°C)	1.8343
k_{He}	Thermal conductivity of the helium gap	(W/m.°C)	0.3143
k_{clad}	Thermal conductivity of the cladding	(W/m.°C)	13.6
c_p	Specific heat at constant pressure	(J/Kg.°C)	5749.5
μ	Water dynamic viscosity	(kg/(m.sec))	$8.9E^{-5}$
$\dot{m}$	Coolant mass flow rate	(m^3/hr.)	68100
P_{inlet}	Coolant inlet pressure	MPa	15.5
Q	Core thermal power	MW_{th}	3410
ρ	Average coolant density along the coolant channel	kg/m^3	703.292

It's clear from Figure 10 that the maximum fuel temperature equals 1337.5 K and occurred at Z=0.0203 m from the centre of the fuel rod, while the maximum clad temperature is 653.9568 K at Z=0.704 m from the centre of the fuel rod.

Figure 10 Fuel, ZIRLO and coolant temperature distribution along z-direction

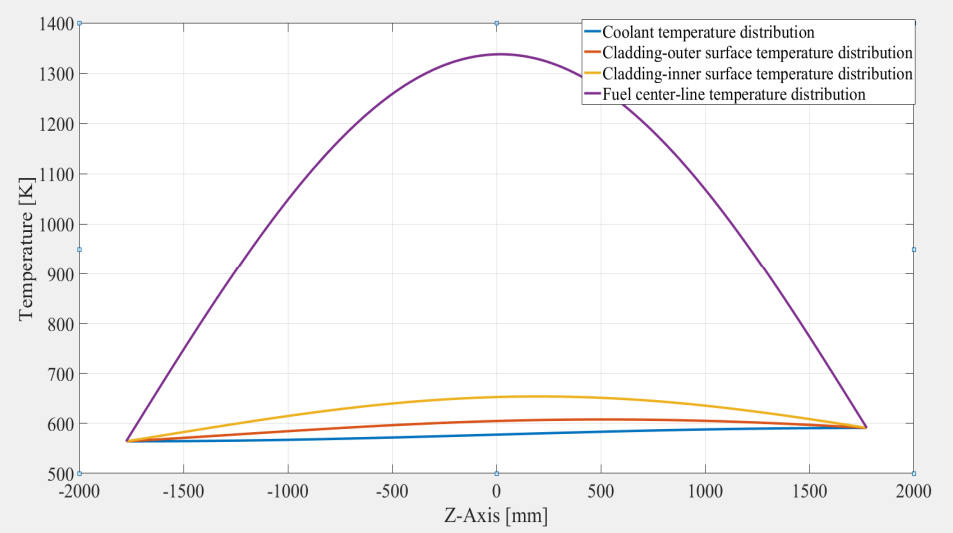

3.2.2 Thermal-hydraulic results using COMSOL-Multiphysics

Computation fluid dynamics is an applied technique for the numerical solution of the different differential equations like (heat generation equation, the Navier-Stokes equation

and Bernoulli's equation, etc.). For this technique, COMSOL-Multiphysics computer software (Comsol, 2013) was used. This software helps in concept-bridging between different branches of physics such as heat transfer, fluid dynamics and solid mechanics. This coupling means that for each node inside the fuel and the cladding materials, a heat generation equation is applied to get the temperature from this temperature. From solving both heat generation equation and the Navier-stokes equation, the stress and strain due to thermal or pressure loads can be simulated. The turbulence model K-Omega has been used to solve the Navier-Stokes partial differential equation numerically. It can be seen from Figure 11(a) how the coolant velocity profile changes along both the axial and radial directions. Figure 11(b) shows the no-slip condition, which describes the variation of the coolant velocity between two statics walls. It can be seen that the absolute velocity of the coolant is zero at the static walls (no-slip condition) then it starts to increase as the coolant become away from the static wall until reaches maximum velocity 3.6 (m/sec) at centre of the coolant channel. This increase in the absolute coolant velocity is due to the decrease in the friction force between the static wall and the coolant layers. Figure 11(c) presents the change of the velocity profile shape along the axial and radial directions. It can be deduced from this figure that the velocity profile shape changes along axial direction from the coolant entrance $Z = 0$ until the fully developed region at $Z = 3.55$ cm, at which the velocity profile shape becomes constant with the change in z-direction. Figure 11(d) shows the coolant pressure drop.

Figure 11 The main results of the solution of the K-Omega turbulence model (a) Velocity profile of the coolant along z-axis in radial direction, (b) The plan view for the velocity profile of the coolant, (c) 2D velocity profile for the coolant along z-axis in radial direction and (d) the coolant pressure drop

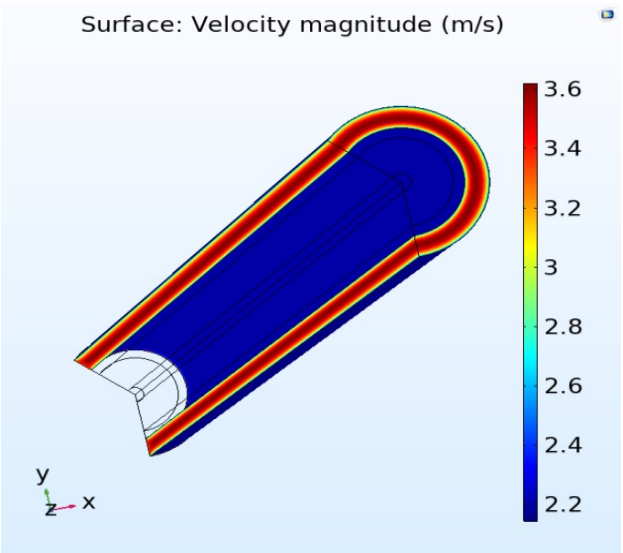

(a)

Figure 11 The main results of the solution of the K-Omega turbulence model (a) Velocity profile of the coolant along *z*-axis in radial direction, (b) The plan view for the velocity profile of the coolant, (c) 2D velocity profile for the coolant along *z*-axis in radial direction and (d) the coolant pressure drop (continued)

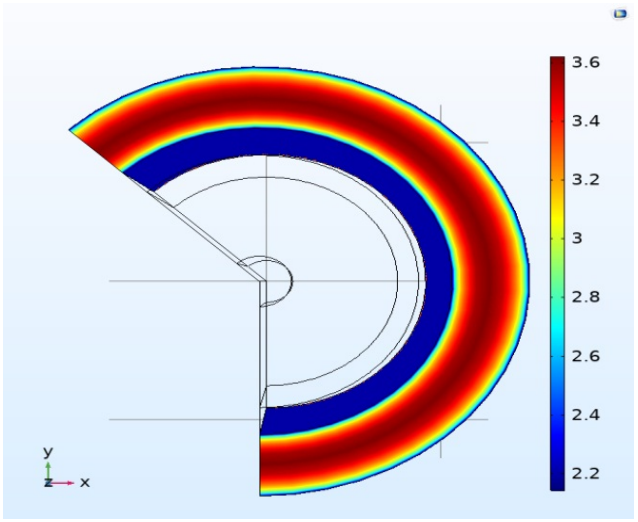

(b)

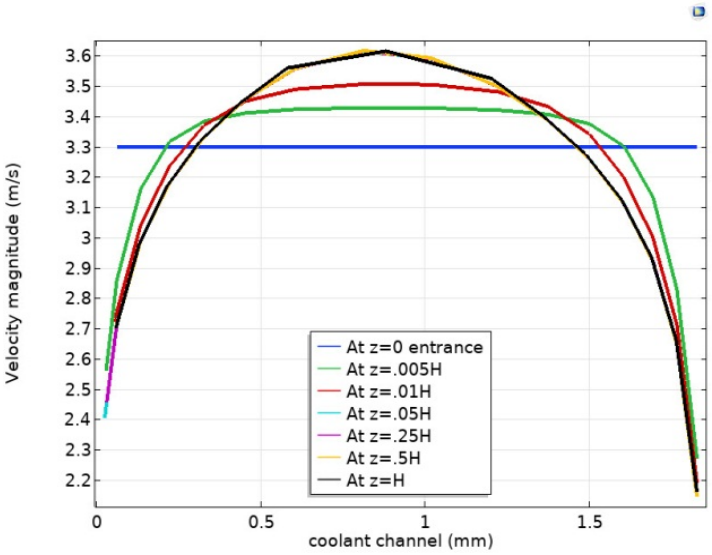

(c)

Figure 11 The main results of the solution of the K-Omega turbulence model (a) Velocity profile of the coolant along *z*-axis in radial direction, (b) The plan view for the velocity profile of the coolant, (c) 2D velocity profile for the coolant along *z*-axis in radial direction and (d) the coolant pressure drop (continued)

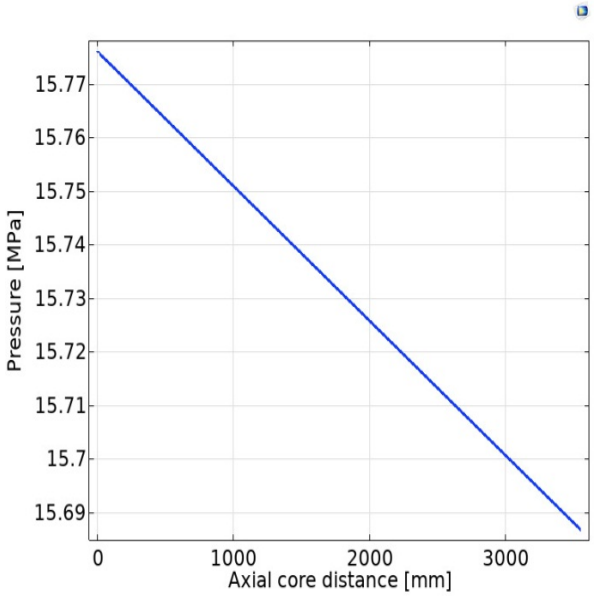

(d)

For solving the heat generation partial differential equation, the following correlations have been used to describe the thermophysical properties of both the fuel and clad materials. These correlations show the effect of the temperature on the thermo-physical properties and the solid mechanics properties for these materials as shown in Table 7. For water and helium, these correlations are existing in the software library.

Table 7 The correlations used for describing fuel and cladding material in the COMSOL program

Property	*Correlation*	*units*
Fuel material (UO_2)		
Thermal conductivity	$k_{.95} = \frac{1}{A + BT + a.gad + f(Bu)} + \frac{E}{T^2} e^{\frac{-F}{T}} + \left[1 - .9 \times e^{-.04\,Bu}\right] g(Bu) \times h(T)$ (Kazimi and Todreas, 1990)	W/ (cm.K)
Heat capacity at constant pressure	$c_p = c_2 + 2c_3 t + 3c_4 t^2 + 4c_5 t^3 + 5c_6 t^4 - c_7 t^{-2}$ (Fink, 2000)	J/ (mole. K)

Table 7 The correlations used for describing fuel and cladding material in the COMSOL program (continued)

Property	*Correlation*	*units*
Density	$\rho(T)=\rho_{\circ}\times(K_i)^{-3}$ $K_i=.99672+1.179\times10^{-5}\times T-2.429\times10^{-9}\times T^2+1.219\times10^{-12}\times T^3$ (IAEA, 2009) $\rho_{\circ}(273)=10.96\,Kg/m^3$	kg/m^3
Young`s modulus	$(217.24\pm4.01)(1-1.92\times P)$ (Marlowe, 1969) P is the volume fraction of the porosity of UO_2	GPa
Poison`s ratio	$\mu=\left(1.323\times\left[\frac{(1-1.92\times P)}{(1-1.66\times P)}\right]-1\right)$ (Marlowe, 1969) P is the volume fraction of the porosity of UO_2	----
Thermal expansion coefficient	$\frac{\alpha(T)}{\alpha(273)}=.99672+1.179\times10^{-5}\times T-2.429\times10^{-9}\times T^2+1.219\times10^{-12}\times T^3$ (IAEA, 2009) $\alpha(273)$ is the linear thermal expansion at T=273 which equal to 9.75×10^{-6}	1/K
Cladding material (ZIRLO)		
Thermal conductivity	$k=23.5-.0192\times T+1.86\times10^{-5}\times T^2$ (IAEA, 2009)	W/ (m.K)
Heat capacity at constant pressure	$c_p=238+.159T$ (IAEA, 2009)	J/ (kg. K)
Density	$\rho(T)=6636-.286T$ (IAEA, 2009)	kg/m^3
Young's modulus	99.3	(GPa)
Poison's ratio	0.37	----
Thermal expansion coefficient	$\alpha(T)=(5.22+1.82*10^{-3}T)10^{-6}$ (IAEA, 2009)	1/K

It can be deduced from Figure 12 that the maximum fuel centre line temperature equals to 1040.04 K, which is lower than the solidus temperature of uranium dioxide. As well as the maximum clad temperature is 625.03 K, which is less than its melting point, 2123 K, as recommended.

Figure 12 Fuel, ZIRLO and coolant temperature distribution in both (a) 3D direction and (b) axial direction

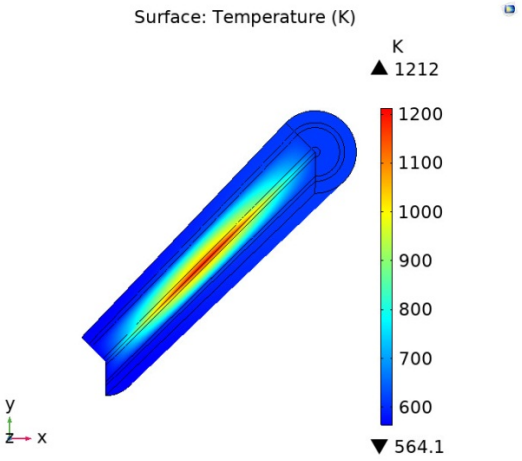

(a)

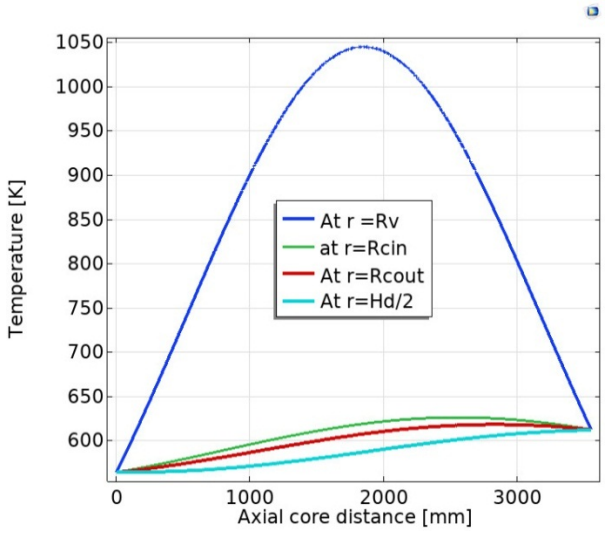

(b)

3.2.3 Calculation of DNBR distribution along the coolant channel in both analytical and CFD approaches

In the thermal-hydraulic analysis, either by analytical or CDF approach, the critical heat flux has been calculated by using EPRI-1 correlation (Kazimi and Todreas, 1990). EPRI-1 correlation was developed by Reddy and Fighetti and it is a function of the inlet quality of the compressed water, the local quality (equivalent quality), the mass flux, the coolant

pressure drop, and the local heat flux. All parameters that are tabulated in Table 8 are measured in British system units (Kazimi and Todreas, 1990).

$$q_{cri}^{``} = \frac{A - x_{in}}{C + \left( \frac{x_e - x_{in}}{q_l^{``}} \right)} \tag{6}$$

where $A = p_1 p_r^{p_2} G^{(p_5 + p_7)}$ & $C = p_3 p_r^{p_4} G^{(p_6 + p_8)}$

Constant	p_1	p_2	p_3	p_4
Value	.5328	.1212	1.6151	1.4066
Constant	p_5	p_6	p_7	p_8
value	–.304	.4843	–.3285	–2.0749

Table 8 The parameters used in the EPRI-1 correlation

Parameter	*Symbol*	*Unit and description*	*Parameter*	*Symbol*	*Unit and description*
Local heat flux	q_l''	$\frac{MBtu}{h.ft^2}$	Thermal power	$\dot{q}$	$\frac{MBtu}{h}$
Equilibrium quality	x_e	$x_e = x_{ein} + \frac{\dot{q}}{2\dot{m}h_{fg}}\left(sin\left(\frac{\pi z}{H} \right) + 1 \right)$	Evaporation enthalpy of the water	h_{fg}	–
Pressure ratio	P_r	the ratio between the system pressure and the critical pressure	Local inlet quality	x_{ein}	–
Critical pressure	P_{Cri}	22.04 MPa	The inlet quality of the compressed water	x_{in}	$x_{in} = \frac{\left(h_{in} - h_f \right)}{h_{fg}}$

It is clear from Figure 13(a) that the MDNBR after using the pressure drop that calculated analytically by using the one-dimensional Bernoulli's equation for vertical tubes is 2.04. on the other hand, after using the coolant pressure drop that calculated numerically by using the turbulence model K-Omega, the MDNBR equals 2.0784 as shown in Figure 13(b).

3.3 Solid mechanic results

Figure 14 presents that the maximum von Mises stress acting on the fuel and the cladding materials are equal to 91.5369 MPa and 40.82 MPa, respectively. The maximum allowable yield stress for the fuel and the cladding materials are 147.1 MPa and 152 MPa, respectively. Figure 15 illustrates the maximum displacement for the fuel material is about 0.06023 mm, which is less than the helium gap thickness between the fuel and the clad materials (0.08 mm), and hence means that no surface contact will occur between the fuel and the clad during at the beginning of the fuel cycle (BOC).

Figure 13 DNBR distribution along *z*-direction based on (a) analytical solution and (b) numerical solution for the coolant pressure drop

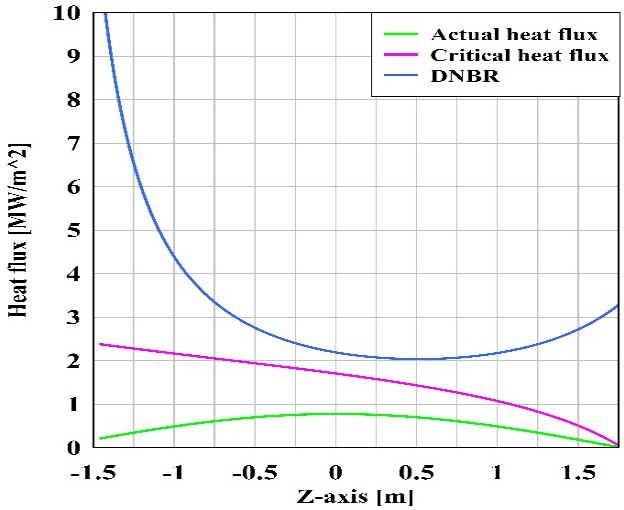

(a)

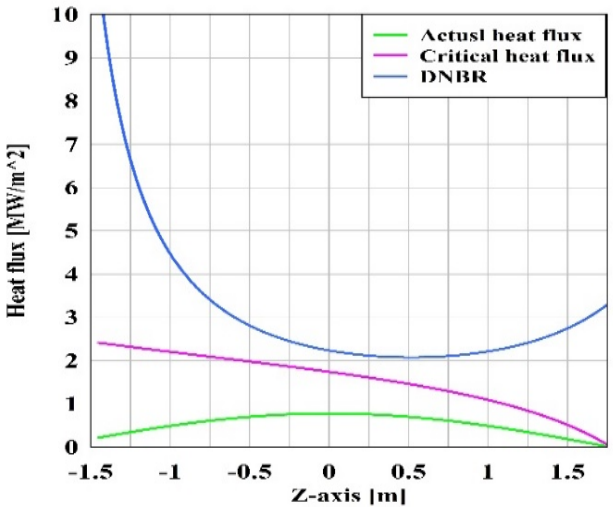

(b)

Figure 14 Surface and volume plots for von Mises stress

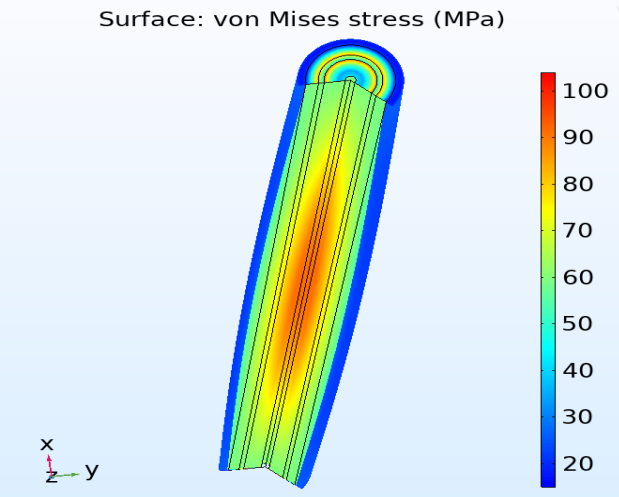

Figure 15 Total displacement for the fuel and the cladding material

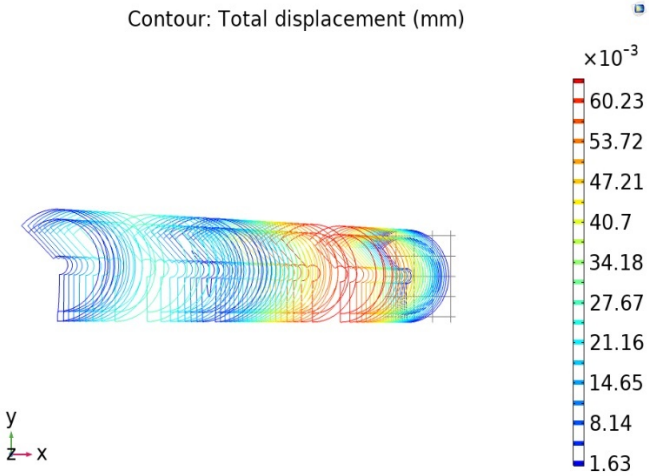

Table 9 illustrates the summary of the obtained thermal-hydraulic and solid mechanics results and compared them with other published works that use WIMS D-4/citation for the neutronic analysis and COPERA-EN (analytical approach) for the thermal-hydraulic analysis (Arshi et al., 2010). The reason for the deviation between the results obtained by COMSOL-Multiphysics and that obtained by either MATLAB or COPERA-EN is that in the analytical solution, approximated values for the thermo-physical properties of the fuel, clad, helium and coolant materials has been used. While in COMSOL-Multiphysics, the correlations that describe the change of the thermo-physical properties of materials with the temperature has been used, which simulate the real situation.

Table 9 The obtained thermal-hydraulic and solid mechanics results summary

Physics	*Parameter*	*COBRA-EN code (Arshi et al., 2010)*	*MATLAB results*	*Relative error %*	*COMSOL results*	*Safety limit of each parameter*
Heat transfer	Max fuel inner surface temperature (K)	1587.5	1398.9	11.88	1040.04	Less than solidus point 2873 K in LWRs (Kazimi and Todreas, 1990)
	Z_m from the centre of the rod (cm)	–	2.03	–	7.071	–
	Max ZIRLO inner surface temperature (K)	653.1	653.95	0.13	625.03	Less than melting point 2123 K
	Z_c from the centre of the rod (m)	–	0.704	–	.72725	–
	Coolant outlet temperature (K)	601.79	590.94	0.72	610.82	In the average of 599.8 K for PWR (Kazimi and Todreas, 1990)
	MDNBR	2.164	2.040	5.68	2.07	MDNBR should be greater than 1.75, according to the FSAR
	Position of MDNBR (m) from the coolant entrance	2.307	2.29	0.65	2.28	–
Fluid dynamics	Velocity profile (m/sec)	$V_{avg} = 3.3006$	$V_{avg} = 3.3006$	–	Fig. 11	–
Solid mechanic	Max Von Mises stress acting on fuel in MPa.	–	–	–	91.81	Less than the fuel yield stress which is about 147.1 MPa (Haase, 1986)
	Max Von Mises stress acting on clad in MPa.	–	–	–	40.82	Less than the ZIRLO yield stress which is about 152 MPa
	Total fuel outer surface displacement in mm	–	–	–	0.06023	–

4 Conclusion

In this work, the neutronic, thermal-hydraulic and solid mechanics analyses have been investigated. The obtained results from the neutronic analysis are the fuel cycle is about 300 days with a maximum fuel burn-up equal to 13.75 GWD/MTU. The neutronic analysis's results show a good agreement with the FSAR. In addition, the results of the thermal-hydraulic analysis conducted using both MATLAB and COMSOL-Multiphysics, show that the maximum temperatures for the fuel and clad also don't exceed the safety limits according to the FSAR. Moreover, the MDNBR values are higher than the safety limits, which assures the impossibility of the coolant phase change. From the solid mechanics analysis, the maximum von Mises stresses acting on the fuel and clad materials were less than their corresponding yield stress. Also, the surface contact between the fuel and the clad materials will not happen because the maximum displacement for the fuel material is about 0.06023 mm, which is less than the helium gap thickness (0.08 mm). The thermal-hydraulic solution using MATLAB saves time and cost and also gives a high degree of acceptance with the FSAR. Also, this study reinforces the use of the COMSOL-Multiphysics computer software in the numerical solution for the thermal-hydraulic and solid mechanics analysis for nuclear power reactors because its results are very consistent with the FSAR.

Acknowledgement

The authors of this paper would like to express their thanks and appreciations to Prof. Amgad Shokr of IAEA for the discussions of the first draft of this work.

References

Arshi, S.S., Mirvakili, S.M. and Faghihi, F. (2010) 'Modified COBRA-EN code to investigate thermal-hydraulic analysis of the Iranian VVER-1000 core', *Progress in Nuclear Energy,* Vol. 52, pp.589–595.

Comsol (2013) *COMSOL Multiphysics 4.3b, User's Guide*.

COMSOL-Multiphysics (2020) *COMSOL Documentation*. Available online at: https://doc.comsol.com/5.6/docserver/#!/com.comsol.help.comsol/helpdesk/helpdesk.html

Faghihi, F., Fadaie, A.H. and Sayareh, R. (2007) 'Reactivity coefficients simulation of the Iranian VVER-1000 nuclear reactor using WIMS and CITATION codes', *Progress in Nuclear Energy,* Vol. 49, pp.68–78.

Faghihi, F., Mirvakili, S.M., Safaei, S. and Bagheri, S. (2016) 'Neutronics and sub-channel thermal-hydraulics analysis of the Iranian VVER-1000 fuel bundle', *Progress in Nuclear Energy,* Vol. 87, pp.39–46.

Faghihi, F.M. and Mohammad, S. (2011) 'Shut-down margin study for the next generation VVER-1000 reactor including 13×13 hexagonal annular assemblies', *Annals of Nuclear Energy,* Vol. 38, No. 11, pp.2533–2540.

Fink, J.K. (2000) 'Thermophysical properties of uranium dioxide', *Journal of Nuclear Materials*, Vol. 279, pp.1–18.

Haase, V. et al. (1986) *U Uranium*.

IAEA (1995) *In-Core Fuel Management Code Package Validation for WWERs*, IAEA-TECDOC-847, International Atomic Energy Agency, Vienna, Austria (November 1995).

IAEA (2009) *Thermophysical Properties of Materials for Nuclear Engineering: A Tutorial and Collection of Data*, INTERNATIONAL ATOMIC ENERGY AGENCY, Vienna.

Kazimi, M.S. and Todreas, N.E. (1990) *Nuclear Systems Volume I: Thermal Hydraulic Fundamentals*, Hemisphere Publishing Corporation.

Lamarsh, J.R. (2020) 'Introduction to nuclear reactor theory / John R. Lamarsh', *SERBIULA (sistema Librum 2.0)*.

Marlowe, A.I.G.K.M.O. (1969) *Ceramic Nuclear Fuel Proceedings of International Symposium*, Washington, DC, Special Pub. No. 2, American Ceramic Society, Columbus, Ohio.

MathWorks, T. (2020) *MATLAB Documentation*. Available online at: https://www.mathworks.com/help/matlab/

McKinney, G. (2011) *MCNPX User's Manual, Version 2.7.0*.

Mohsen, M.Y.M., Soliman, A.Y. and Abdel-Rahman, M.A.E. (2020) 'Thermal-hydraulic and solid mechanics safety analysis for VVER-1000 reactor using analytical and CFD approaches', *Progress in Nuclear Energy*, Vol. 130. Doi: 10.1016/j.pnucene.2020.103568.

ROSATOM (2020) *Modern Reactors of Russian Design*. Available online at: https://www.rosatom.ru/en/rosatom-group/engineering-and-construction/modern-reactors-of-russian-design/index.php?sphrase_id=1493737

Wikipedia (2020) *VVER*. Available online at: https://en.wikipedia.org/wiki/VVER#VVER-1000